O. Oni and C. Bathias**

Fatigue Crack Growth in Micro-notched Specimens of High Strength Steels

REFERENCE Oni, O. and Bathias, C., **Fatigue Crack Growth in Micro-notched Specimens of High Strength Steels**, *The Behaviour of Short Fatigue Cracks*, EGF Pub. 1 (Edited by K. J. Miller and E. R. de los Rios) 1986, Mechanical Engineering Publications, London, pp. 295–307.

ABSTRACT Small fatigue crack formation and growth, from single-edge micro-notched specimens of high strength low alloy martensitic steels, were studied under pure bending and constant amplitude loading conditions, employing a carefully calibrated pulsed direct current electric potential technique.

It was observed that small cracks formed sporadically along the notch root, and that their growth rate was different from long through-cracks. The growth rate of the small cracks fell to a minimum before rising again, to join with the long through-crack growth curve determined on conventional specimens. The observed short crack depth varies from a few microns to approximately 900 microns from the notch root.

Introduction

Very recently the study of short or small part-through fatigue cracks has attracted considerable attention, not only because of its academic interest but also because of its practical implications in design, as they are generally the origin of most structural failures.

Observations made during fatigue experiments have shown that this type of crack propagates at rates different from long through-cracks subjected to the same nominal crack driving force (**1**)(**2**) and, furthermore, they can also grow under stress intensity conditions that are below the threshold stress intensity factor range, ΔK_{th}, determined from long through-cracks in conventional specimens (**3**)(**4**).

The principal reasons advanced to explain these observations include plasticity effects, crack closure phenomena, the breakdown of linear elastic fracture mechanics analysis in the short crack region, non-equilibrium crack profiles, and the decrease in stress concentration factor with distance from a notch root (**3**)(**5**).

In this paper we report part of our current experimental observations on the formation and the growth of small part-through fatigue cracks, emanating from single edge micro-notched (SEN) bend specimens of high yield strength martensitic steels. The pulsed direct current (d.c.) electric potential technique was used for the detection and the continuous measurement of crack growth. The results on the growth of the part-through fatigue cracks, were compared with those of long through-cracks determined from conventional compact tension specimens.

* Laboratoire de Mécanique – UA, 849 du CNRS, Université de Technologie de Compiègne, B.P. 233. 60206 – Compiègne. France.

Table 1 Percentage weight composition of the materials

Steel type	*C*	*Si*	*Mn*	*S*	*P*	*Cr*	*Ni*	*Mo*	*Cu*	*Al*
16 NCD 13	0.16	0.28	0.48	<0.03	<0.09	0.96	3.14	0.23	0.10	—
30 NCD 16	0.27	0.22	0.38	0.005	0.005	1.30	3.79	0.44	0.16	0.006

Table 2 Heat treatments and mechanical properties

Material	*Heat treatment*	*0.2% yield strength* σ_{ys} (MPa)	*Ultimate tensile strength* σ_{ult} (MPa)	*Elongation* (%)
16 NCD 13	Austenized at 825°C for 0.5 h oil quenched and tempered at 190°C for 2 h	1070	1360	13
30 NCD 16	Austenized at 850°C for 0.5 h oil quenched, tempered at 585°C for 1 h	1076	1192	15.3

Experimental procedure

Material

Two similar nickel chromium martensitic steels, types 16 NCD 13 and 30 NCD 16 of the French standards, principally used in the aeronautical industry, were used in the present investigation. Their chemical composition, heat treatments, and mechanical properties are presented in Tables 1 and 2. The average grain size of the steel 30 NCD 16 is about 30 μm while that of 16 NCD 13 is of the order of 25 μm.

Specimen preparation

Single edge notched specimens having nominal dimensions 100 × 20 × 10 mm were machined in the LT direction of the plate (Fig. 1(a)). A small 60 degree V shaped notch, of depth 0.1 mm and root radius ρ = 45 μm, was machined across the 10 mm width by electro-discharge machining. The notch was mechanically polished, first with abrasive paper, and then with alumina paste down to 1 μm. Four pairs of potential probes were positioned as shown in Fig. 1(b). Thin copper wire probes were micro-welded to the specimen surface.

The fatigue crack growth tests were carried out in air, on a ±10 kN Instron fatigue machine at constant amplitude of cycling ($\sigma_{max}/2 = 0.39\sigma_{ys}$, $\sigma_{min}/\sigma_{max} = 0.1$, where σ_{max} is the gross maximum bending stress). The test frequency was 20 Hz and four point bending was applied. The formation of a crack was detected and its growth monitored continuously with a pulsed d.c. electric

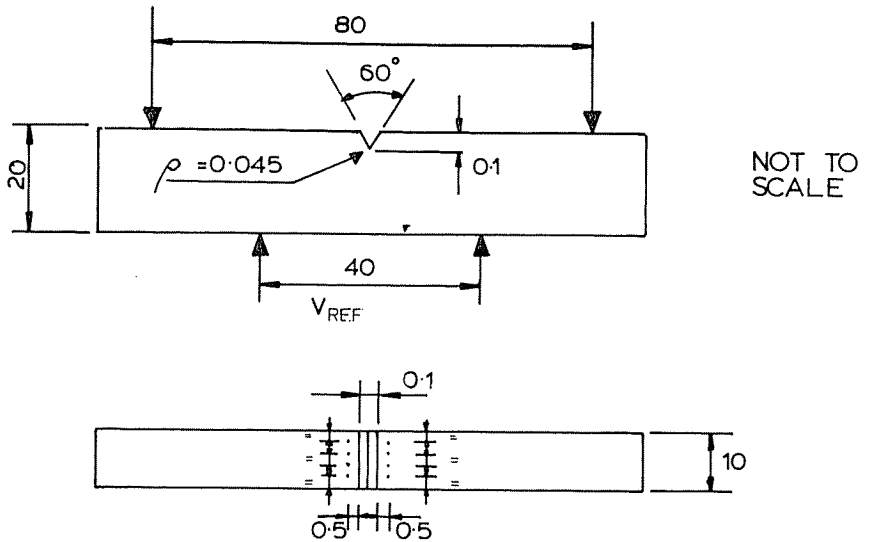

Fig 1 Specimen dimensions and the equi-distance positions of the eight probes near the notch. All dimensions in millimetres (not to scale)

potential technique developed by Baudin and Policella (**6**). A commutator in the electric circuit permitted switching from one probe position to another. Potential drop changes and the number of cycles were continuously recorded. The moment the crack was considered to have propagated significantly, the test was stopped and the specimen broken open under static loading, in order to reveal the crack profile. The fracture surfaces were then observed and the crack dimensions (surface length and depth) measured in the scanning electron microscope (SEM).

Results and discussions

Microscopic observations

Experimental observations, confirmed subsequently by the scanning electron microscope, showed that despite having a continuous small through-thickness micro-notch in the specimen, several small part-through fatigue cracks were sporadically formed along the notch root and their formation was not concentrated at a particular point. The four pairs of potential drop probes therefore facilitated the detection and monitoring of the growth of such cracks at any point along the notch root. Figure 2 shows some of the SEM micrographs of the cracks. In some cases several cracks were observed, each at a different stage in its development (Fig. 2(a)). Regarding the crack shape, the semi-elliptical form

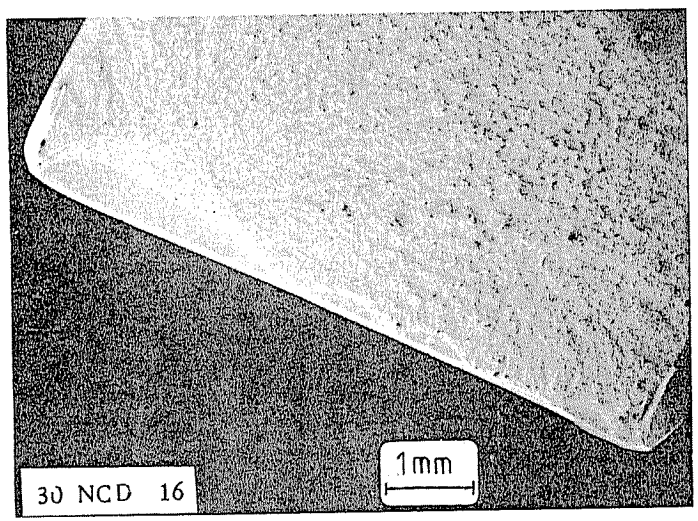

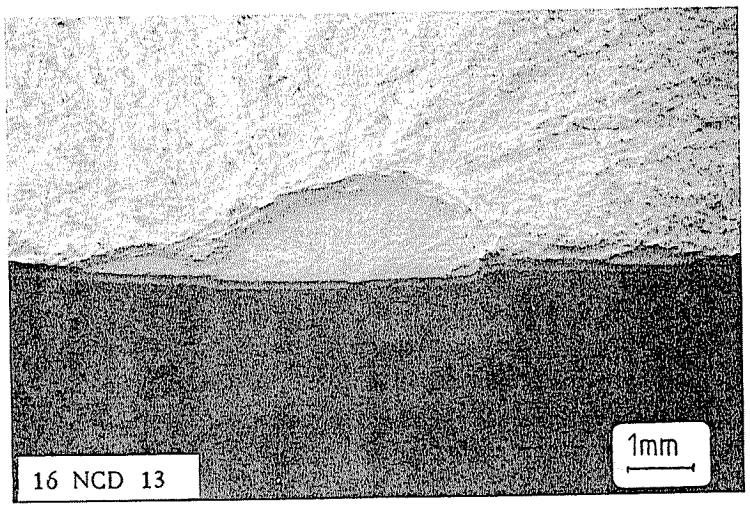

Fig 2 Typical small part-through fatigue cracks emanating from through-thickness micro-notched specimens

was the most common though other shapes were also evident, particularly the quarter ellipse form at specimen corners.

Quantitative microscopic observations revealed that these cracks originated principally from irregularities at the notch root. It is also thought that inclusion pits, formed as a result of the poor adhesion between the aluminium oxide inclusion and the matrix material (**7**), could also contribute to the sporadic formation of small cracks.

Further experimental tests and observations showed that these cracks grew for a large number of cycles as small part-through cracks before coalescing to become a single through-thickness crack, which eventually led to the catastrophic failure of the specimen.

Calibration of the crack length measuring system

The calibration of the potential drop system was carried out as follows The variation in electric potentials was measured by the four pairs of probes which were summed and averaged and then normalized (**6**)(**8**)(**9**) with a reference potential, V_{ref}. Here V_{ref} is the potential difference measured at the beginning of a test at a distance of $2W$ from the centre of the specimen, where W is the specimen width.

The normalized averaged potential difference $\Delta V_m/V_{ref}$ was then plotted as a function of the total cracked area measured from the microscopic observations. Figure 3 shows the calibration curve obtained from several specimens cracked under the same experimental conditions. The curve shows that the electrical potential sensitivity to crack growth is the same in the two steels, though agreement was not perfect; this is expected as the electrical potential sensitivity of a material to crack growth depends on the electrical conductivity and the dimensions of the crack formed in the material (**8**). Since the two materials have similar physical properties, and the dimensions of the cracks formed in the materials were of the same order it is not surprising that their electrical potential sensitivity to crack growth is almost identical.

Crack length and growth analysis

As the objective is to express the average growth rate of these cracks in terms of the stress intensity factor range, the following assumptions were made in order to simplify the analysis.

(1) Linear elastic fracture mechanics analysis is applicable to the short crack problem.
(2) The interaction between cracks is negligible and the biggest of these cracks (in cases where there were several) has the most damaging effect.
(3) The aspect ratio of the crack remains constant.

If these assumptions are valid, then the present results can be analysed by applying the empirical stress intensity factor solutions developed by Raju and

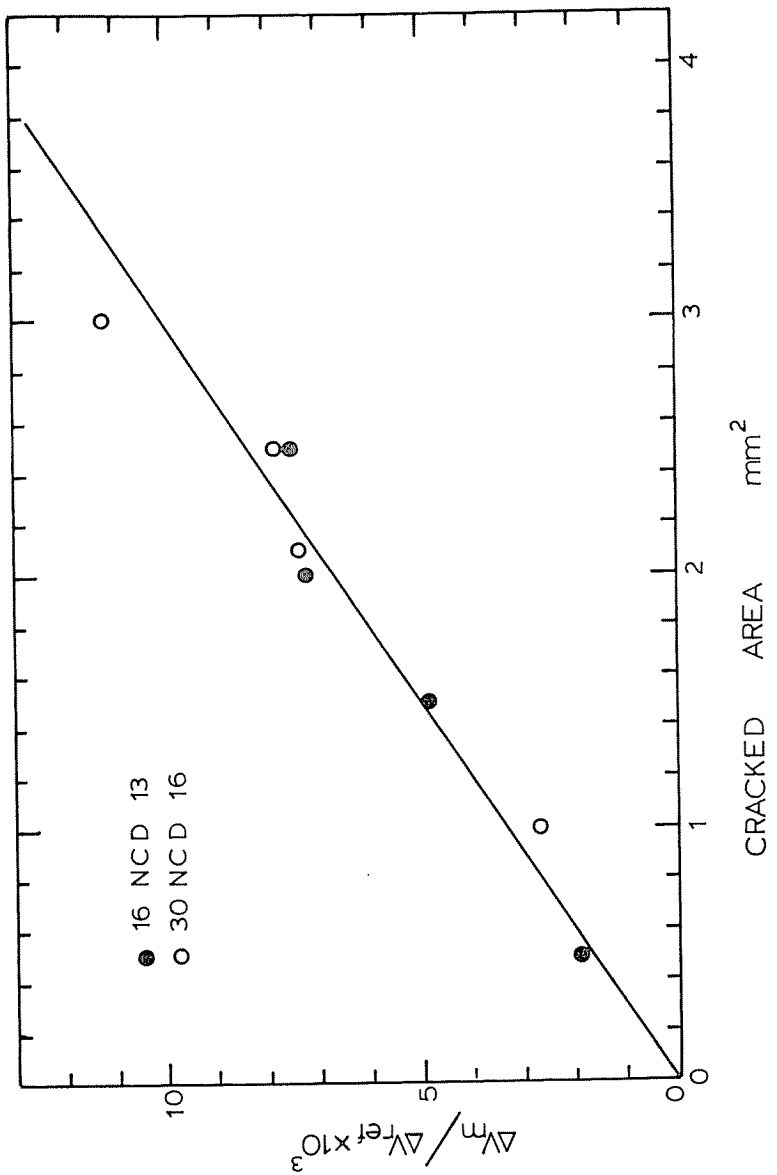

Fig 3 Electrical potential drop calibration for the notch of Fig. 1

Newman (**10**) for surface crack growth under pure bending conditions. The analysis is as follows.

From the calibration curve we obtain an equation of the form

$$\Delta V_m/V_{ref} = AS \tag{1}$$

further, we know that the area, S, of a semi ellipse is given as

$$S = \pi/2 a_i c_i \tag{2}$$

and, finally, from assumption (3) above we have

$$a/c = a_i/c_i = a_{final}/c_{final} = \text{constant} \tag{3}$$

S = crack area
a = depth of crack
c = half of the total surface length of crack
A = constant determined from calibration curve

Equations (1) and (2) are therefore used to calculate the depth and the surface length of the cracks. The minimum detectable crack depth from the notch root measured by the present electrical potential instrumentation was of the order of 30 μm when the crack formed exactly opposite a probe wire, and of 50 μm when it formed in between probe wires. The maximum crack depth measured in this latter case was approximately 900 μm. Furthermore, the calculated crack depths were found to be approximately ± 10 per cent of their actual values in the former case and ± 15 per cent in the latter.

Figure 4 gives crack length values c, in terms of the number of cycles, showing that, at the loading level considered, crack formation takes place earlier in steel 16 NCD 13 than in 30 NCD 16. Detailed experimental results at different loading levels confirm this point. They also show that 30 NCD 16 is characterized by the formation of several more small cracks than 16 NCD 13. The earlier crack formation in the latter is thought to be due to its lower threshold stress intensity factor value of 6 MPa$\sqrt{m}$ for 30 NCD 16 steel.

The ability of 30 NCD 16 steel to form several cracks can be associated with the presence of Al_2O_3 inclusions which, according to a quantitative fatigue crack initiation study carried out by Kunio *et al.* (**7**) on a similar martensitic steel, may initiate cracks at inclusion pits formed due to the poor adhesion between this oxide and the matrix. Since these pits are randomly distributed in the matrix, multiple crack initiation sites would be expected. Scanning electron microscope studies of the crack formation zones near the notch root in the two materials provided some evidence of inclusions on the fractured surface of the 30 NCD 16, while in Fig. 5 the crack is seen to initiate at the site of an irregularity on the notch root, even though some inclusions must be present in this material.

Figure 6 shows the relation between the fatigue crack growth rate in the depth direction, as a function of the stress intensity factor range, for the part through- and the long through-cracks in the two materials.

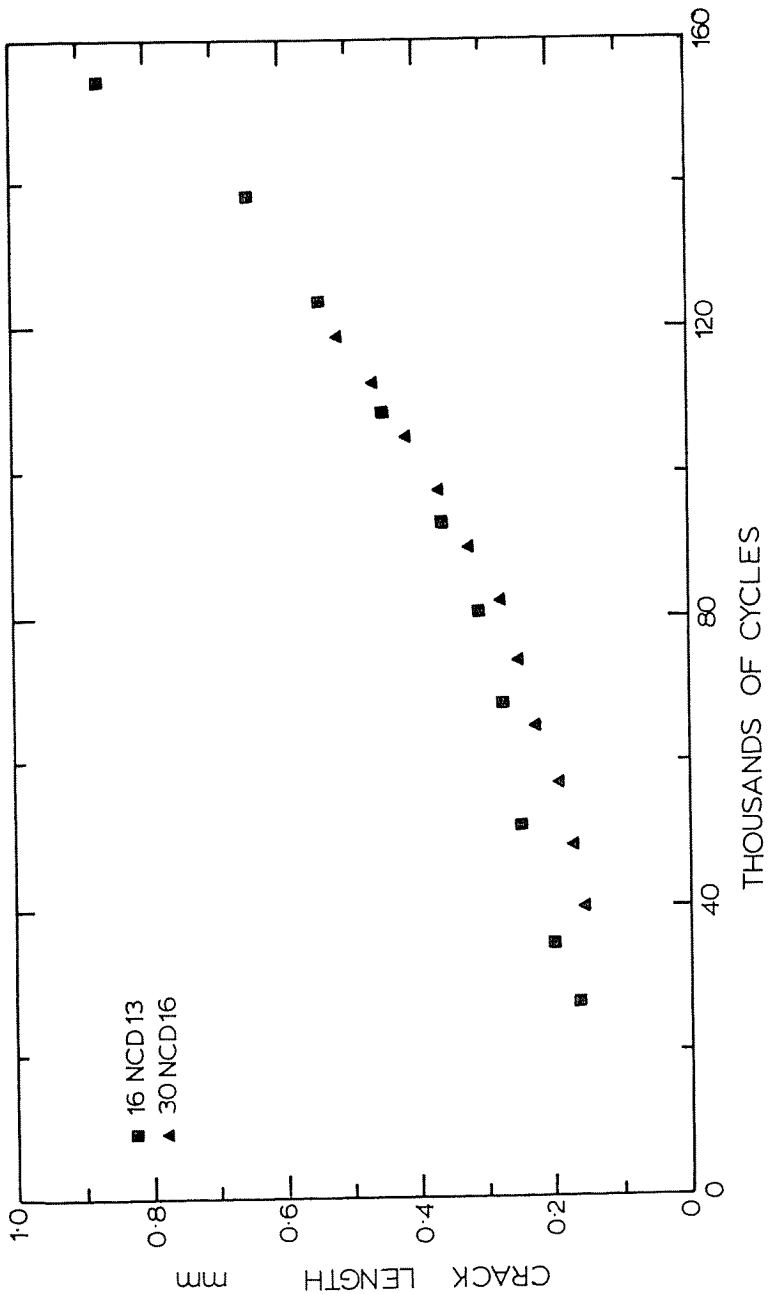

Fig 4 Crack length of a part-through crack in terms of the number of cycles: $R = 0.1, f = 20$ Hz

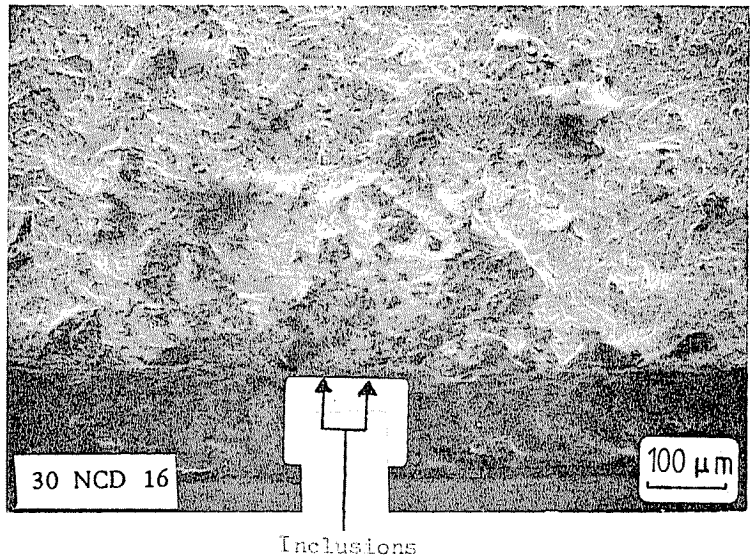

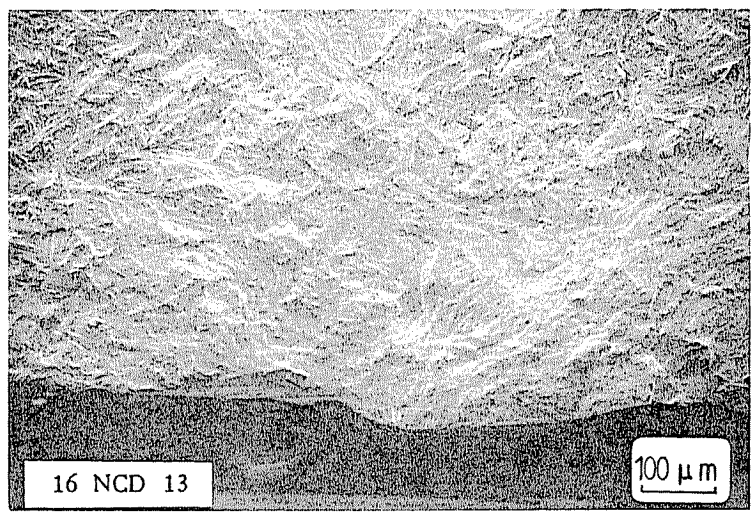

Fig 5 Micro-notch root irregularities

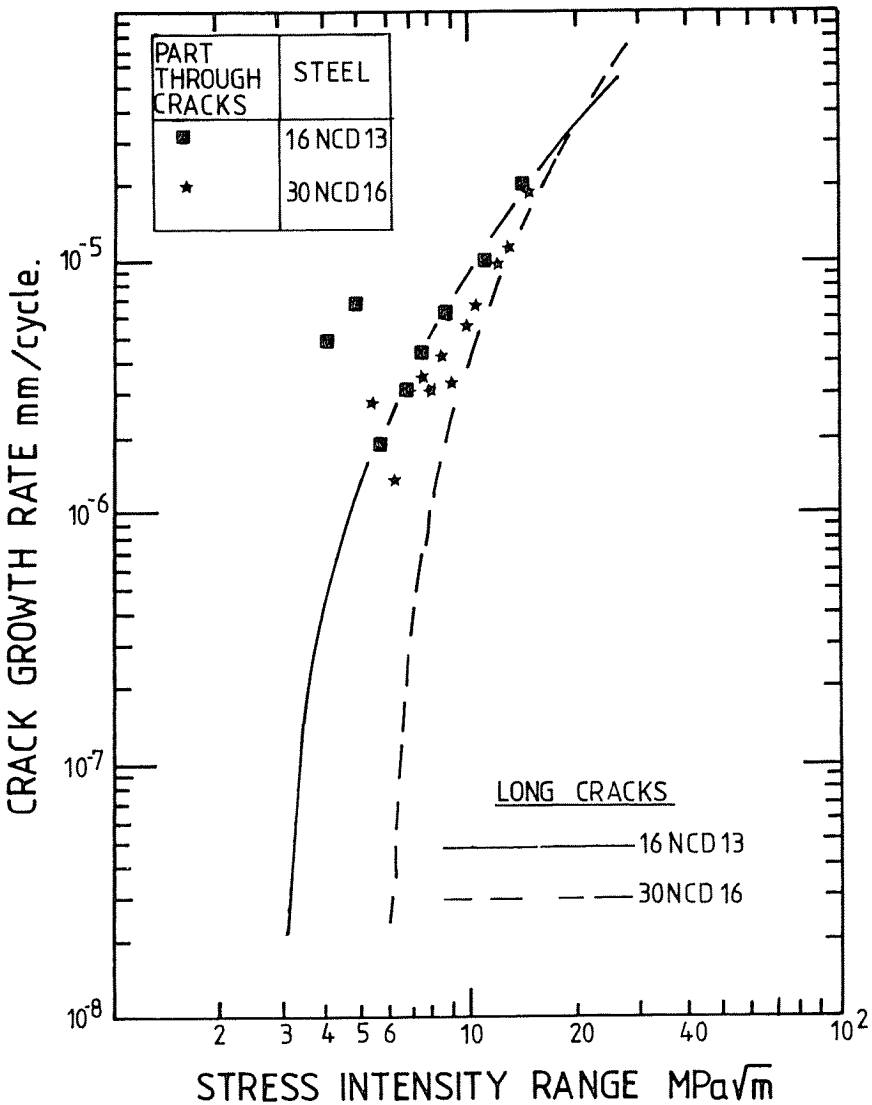

Fig 6 Comparison of crack growth rates in terms of the stress intensity factor range in two steels: $R = 0.1$, $f = 20$ Hz

The long through-crack

The full line and the dashed line of Fig. 6 represent the long through-crack results ($a > 1$ mm) in 16 NCD 13 and in 30 NCD 16 steels, respectively. The experimental data points were omitted for clarity. The data were obtained using compact tension specimens and the near threshold was determined using the load shedding technique. It was found that the value of the threshold stress intensity factor of the material of steel 30 NCD 16 is nearly double that of steel 16 NCD 13 – a surprising result, as the two materials have identical mechanical properties. This further shows that two materials may have similar mechanical properties but not necessarily similar defect tolerance.

The part-through crack

Although some of the experimental data exhibit scatter, especially at very short crack depth or low stress intensity, Fig. 6 indicates that, at very short crack depth, most experimental points lay outside the long through-crack data, indicating a higher propagation rate of the short crack in comparison with the equivalent long through-crack. There is also an initial dip or minimum growth in the two materials. In the case of 16 NCD 13 steel at this minimum point, the short crack data merges with the long through-crack curve, and this point, according to our analysis, corresponds to a crack depth of about 260 μm. In the case of material 30 NCD 16 the minimum point occurs at a lower crack depth (190 μm); moreover, the merger point of the short crack data with the long crack curve is not at this minimum point, but at a crack depth of about 220 μm. Also at very short crack lengths, the ΔK values for steel 16 NCD 13 were higher than the equivalent value of the ΔK at threshold, while for steel 30 NCD 16 the initial ΔK value for the short crack is approximately the same as its threshold stress intensity factor value.

Figure 7 shows our experimental results on the two materials compared with the work of Fine and Heubaum (**5**) on the short crack growth behaviour of a micro-notched ($\rho = 25$ μm) single edge notch specimen of a high strength low alloy steel (HSLAVAN 80) in which the crack length was measured with an optical microscope. Figure 7(a) shows the comparison with the steel 16 NCD 13 while Fig. 7(b) shows the comparison with the steel 30 NCD 16. From the Figs it can be seen that our experimental curves have similar shape to those previously reported in that each curve can be said to go through a minimum before rising up again to join the conventional long-crack growth behaviour. In addition, the short-crack growth behaviour in the three materials takes place at a growth rate of the order of 10^{-6} mm/cycle, and the ΔK values at very short crack length are higher than the equivalent ΔK at the threshold of each material.

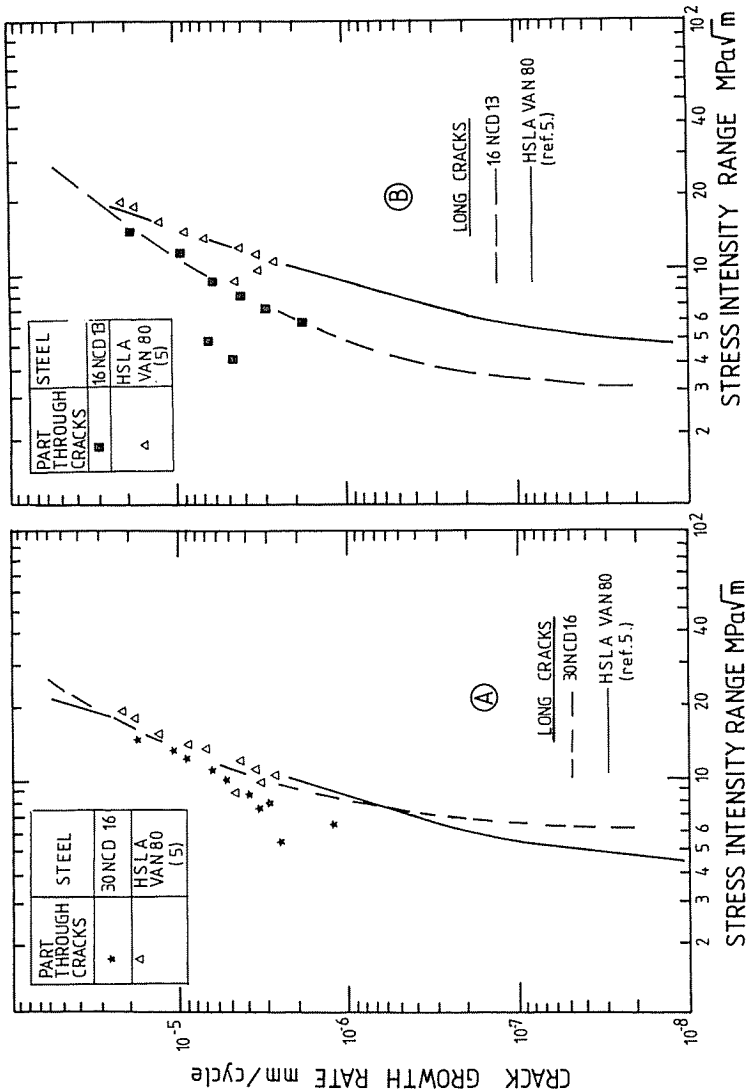

Fig 7 Comparison of the crack growth rate in terms of the stress intensity range in two steels.
(a) 30 NCD 16
(b) 16 NCD 13

Conclusions

Part-through fatigue crack formation and growth were studied in micro-notched specimens of high yield strength low alloy martensitic steels.

Several cracks developed sporadically along the notch root and were of varying shapes and sizes. They originated principally from the irregularity of the notch root. It is also thought that inclusion pits formed as a result of the poor adhesion between aluminium oxide inclusions and the matrix, and these pits were responsible for sporadic crack formation.

The cracks were observed to grow for a large number of cycles as part-through cracks before joining up to form a single through-thickness crack that eventually lead to the failure of the specimen. The growth rate of the several small cracks was also observed to be different from that of equivalent through-cracks measured on conventional compact tension specimens.

The experimental results further confirmed the ability of the direct current electric potential technique to detect and monitor continuously and quantitatively the sub-critical growth of a crack emanating from a small surface defect.

References

(1) GANGLOFF, R. P. (1981) Electrical potential monitoring of crack formation and sub-critical growth from small defects, *Fatigue Engng Mater. Structures*, **4**, 15–33.

(2) NEWMAN, Jr, J. C. (1982) A non linear fracture mechanics approach to the growth of small cracks, Agard Specialist Meeting on Behaviour of Short Cracks, Toronto.

(3) SURESH, S. and RITCHIE, R. O. (1983) The propagation of short fatigue cracks, Report No. RP/83/1014. University of California at Berkeley.

(4) TANAKA, K. and NAKAI, Y. (1983) Propaation and non propagation of short fatigue cracks at a sharp notch, *Fatigue Engng Mater. Structures*, **6**, 315–327.

(5) HEUBAUM, F. and FINE, M. F. (1984) Short fatigue crack growth behaviour in a high strength low alloy steel, *Scripta Met.*, **18**, 1235–1240.

(6) BAUDIN, G. and POLICELLA, H. (1982) A pulsed d.c. P.D. technique applied to three dimensional crack fronts, *Advances in crack length measurements* (Edited by C. J. Beevers), EMAS, Warley, pp. 159–174.

(7) KUNIO, T., SHIMIZY, M., YAMADA, K., SAKURA, K. and YAMAMOTO, T. (1981) The early stage of fatigue crack growth in martensitic steel, *Int. J. Fracture*, **17**, 111–119.

(8) ATKINSON, E. C. and SMITH, M. E. F. (1982) The detection and measurement of non-through cracks using the A.C. potential difference method, National Gas Turbine Establishment Memorandum, M. 81001.

(9) GANGLOFF, R. P. (1982) Electrical potential monitoring of the formation and growth of small fatigue cracks in embritting environments, *Advances in crack length meauerements* (Edited by C. J. Beevers) EMAS, Warley, pp. 174–229.

(10) NEWMAN, Jr, J. C. and RAJU, I. S. (1984) Stress intensity factor equations for cracks in three dimensional finite bodies subjected to tension and bending loads, 19827 NASA Technical Memorandum.